Contract No:

This document was prepared in conjunction with work accomplished under Contract No. 89303321CEM000080 with the U.S. Department of Energy (DOE) Office of Environmental Management (EM).

Savannah River National Laboratory®

A U.S. DEPARTMENT OF ENERGY NATIONAL LAB • SAVANNAH RIVER SITE • AIKEN, SC • USA

2022 Report - SRNL Aging and Lifetimes program tritium aging studies on structural alloys

Timothy M. Krentz

Anastasia Mullins

January 2023

SRNL-STI-2023-00001, Revision 0

DISCLAIMER

Printed in the United States of America

Prepared for
U.S. Department of Energy

Keywords: *Mechanical Properties, Type 304L Stainless Steel, Type 21-6-9 Stainless Steel, Hydrogen, Tritium, Helium, Embrittlement*

Retention: *Permanent*

2022 Report - SRNL Aging and Lifetimes program tritium aging studies on structural alloys

Timothy M. Krentz
Anastasia Mullins

January 2023

Savannah River National Laboratory is operated by Battelle Savannah River Alliance for the U.S. Department of Energy under Contract No. 89303321CEM000080.

REVIEWS AND APPROVALS

AUTHORS:

____

Timothy M. Krentz, GAS TRANSFER SYSTEMS TECHNOLOGY GROUP Date

____

Anastasia Mullins, GAS TRANSFER SYSTEMS TECHNOLOGY GROUP Date

TECHNICAL REVIEW:

____

Daniel Morrall, GAS TRANSFER SYSTEMS TECHNOLOGY GROUP, Reviewed per E7 2.60 Date

APPROVAL:

____

Scott L. West, GAS TRANSFER SYSTEMS TECHNOLOGY GROUP Date

____

M. Lane Rogers, Manager Date
GAS TRANSFER SYSTEMS TECHNOLOGY GROUP

PREFACE OR ACKNOWLEDGEMENTS

Joe Ronevich of Sandia National Laboratories provided specimens used for tritium pre-charging. He also contributed testing results on hydrogen exposed samples, as well as valuable technical discussion and feedback. Thomas Warren and Kellie Holland performed Material Control and Accountability activities. Stephanie Crossland, Chad Sweeney, Calvin Clamp, Anne Kelly, Dante Pilgrim, and Mauricio Martinez helping in preparing tritium charging vessels and tritium charging procedures; conducting specimen recovery; and transporting specimens to SRNL after tritium pre-charging runs. Gavin Mattingly assisted with mechanical testing, and Dale Hitchcock and Daniel Morrall provided technical review.

EXECUTIVE SUMMARY

This report documents work performed in fiscal year 2022 at SRNL in support of the Aging and Lifetimes program. This work is an enduring collaboration between SRNL and SNL to study tritium embrittlement of structural metals used in Gas Transfer System reservoirs. The measured data inform component lifetime assessments and predictions. Test coupons are thermally pre-charged with tritium and allowed to age at cryogenic temperatures to freeze out tritium diffusion and minimize off-gassing while allowing for decay helium levels to build. Coupons are removed and tested at planned intervals to measure how mechanical properties degrade as helium levels increase. This report summarizes test results from coupons which are in various stages of aging as they were tritium pre-charged in previous years, as well as documenting one new charging run.

304L stainless steel that was previously tritium pre-charged and allowed to age to nominally 650 appm helium was tested with previous testing conducted at 100 and 300 appm helium content. Tensile testing of heat treated 304L tubes (and welded tubes) aged to 3 increasing helium levels completes a unique study of a diverse set of microstructures and yield strengths ranging from 200-800 MPa. Additionally, notched and smooth 304L tensile specimens aged to 650 appm helium were tested to predetermined strains to provide for a systematic microscopy investigation of aging effects on deformation mechanisms. 304L electron beam (EB) weld coupons and annealed 21-6-9 coupons were also tested at 300 and 680 appm helium content respectively. Table 0-1 provides the status of the ongoing tritium coupon aging studies.

Table 0-1. Status of Ongoing Tritium Coupon Aging Programs

		Mechanical Testing of Aged Specimens with Born-in Helium (appm)				
Material	**Tritium Pre-charged (year)**	**100**	**200**	**300**	**600**	**1000**
304L weld/HAZ	2017	DNM	NP	Complete	Complete	Planned
21-6-9 weld/HAZ*	2017	DNM	NP	Complete	Complete	Planned
304L tube, tensile	2019	Complete	NP	Complete	Completed[1]	Planned
304L E-beam welds	2020	Complete	NP	Completed	Planned	Planned
21-6-9 Annealed	2020	Complete	Complete	Complete	Completed[2]	Planned
AM[3] 304L and 316L	2022	Planned	Planned	Planned	Planned	NP

DNM = did not measure
NP = not planned
Completed = new testing completed in 2022
**21-6-9 HAZ has higher tritium solubility than 304L and thus reaches relevant Helium concentrations in shorter aging times*
[1,2]Testing was delayed ~3 months, leading to approximately [1] – 650 and [2] – 680 appm helium
[3] Additively Manufactured

TABLE OF CONTENTS

LIST OF TABLES

LIST OF FIGURES

LIST OF ABBREVIATIONS

SRNL	Savannah River National Laboratory
SNL (/CA)	Sandia National Laboratories (California campus)
FZ	Fusion Zone (as of a weld)
HAZ	Heat Affected Zone (as of a weld)
appm	Atomic parts per million
AM	Additive Manufacturing

1.0 Introduction

Pressure vessels for tritium storage are constructed from forged austenitic stainless steels. These materials of construction provide compatibility with hydrogen isotopes. Nonetheless, some embrittlement does occur when hydrogen and its isotopes, including tritium, dissolve into the metal's atomic lattice and alter deformation processes. Over time, tritium decays to relatively insoluble helium, creating immobile nanoscale bubbles that progressively reduce fracture resistance as helium contents increase. The consequences of a leak in service are high, and SRS handles some tritium containing components at the end of their service life, thus having a vested interest in their structural integrity. Cracks have been observed in storage vessels after extended service [1-5]. Predicting safe service life requires measurements of the impacts of aging on mechanical performance. Savannah River National Laboratory's (SRNL's) program on tritium impacts on structural materials provides data on the properties of stockpile relevant materials as they age in tritium to inform lifetime assessment and prediction for tritium storage vessels.

Tritium embrittlement has been studied at SRNL through tensile and fracture mechanics testing of austenitic stainless steel forgings, providing empirical basis for design [6, 7]. Data on stockpile forgings as well as variations on forging methodologies and welds, combined with testing at SNL/CA on hydrogen-pre-charged materials, have provided the basis for the modern understanding of hydrogen-isotope embrittlement. SRNL's present work with SNL/CA aims to further understanding of tritium embrittlement and provide the experimental data necessary to develop quantitative models of tritium embrittlement and predict component lifetimes.

The above-mentioned historical studies have informed the design of ongoing work. As they advanced from representative material studies to engineering studies on forgings and joining technology in service, current investigations take a strategy of meeting data requirements necessitated by changing manufacturing technologies and progressing on to microstructural characterizations which further understanding of structure-process-properties-performance relationships exhibited by materials after tritium aging. Testing this year completed a systematic experiment on the sensitivity to tritium embrittlement of varying microstructures in 304L stainless steel tubing and orbital welds. Data on flow curves, plastic deformation, and triaxial stress states in 304L stainless steel after tritium exposure and aging was measured from smooth and notched tensile test specimens. Tensile testing and fracture testing of electron beam (EB) welded 304L stainless steel after tritium exposure was continued, and the tensile response of annealed 21-6-9 stainless steel at higher helium contents was also measured. These data provide insights on the performance of EB welds, used in future GTS reservoir designs, and help to explain large losses observed fracture resistance in the fusion zones (FZ) and heat affected zones (HAZ) of 21-6-9 stainless steel welds.

2.0 Experimental Procedure

2.1 Testing of Type 304L Electron Beam Welded Material

SRNL-STI-2021-00046 [8] describes the preparation and thermal pre-charging with tritium of EB weld 304L stainless steel specimens. SRNL-STI-2022-00001 [9] presents initial testing at 100 appm nominal helium content. Fracture resistance and tensile tests on 304L stainless steel EB weld specimens were conducted at room temperature in air using a screw-driven testing machine in displacement control while measuring load, crosshead displacement, and extension. Crack opening displacement via clip on gage, and electrical potential drop for determination of crack extension were measured for the fracture resistance tests. Drawings of the specimen geometries are shown in Figure 2-1. Figure 2-2 displays an image of a fracture specimen under test. Tests described here were conducted 18 months after the initial tritium thermal pre-charge to allow the specimens to develop nominally 300 appm internal helium.

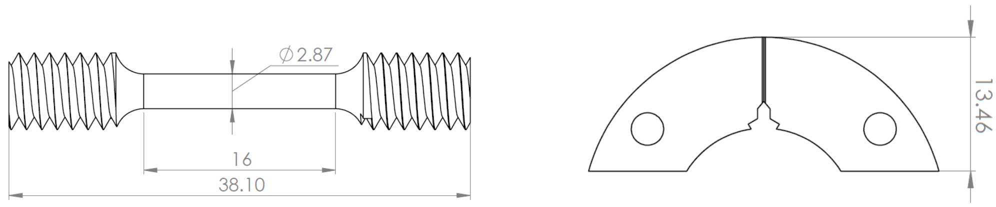

Figure 2-1 – Drawings of threaded tensile specimens (left) and arc shaped fracture mechanics specimens (right). Dimensions in mm

Figure 2-2 – Testing Configuration for Arc shaped fracture mechanics specimens

2.2 Type 304L Stainless Steel Specimens

2.2.1 304L Stainless Steel Tube Specimens

Strain-hardened 304L stainless steel tubing was heat treated to create a series of microstructures and strengths with identical composition. Details on the heat treatment, thermal pre-charging with tritium, and initial testing can be found in [8, 10-12]. Information on the preparation and results of testing samples in the non-charged and hydrogen-pre-charged condition are described in [10, 11]. The test setup can be seen in the left panel of Figure 2-3.

Figure 2-3. SRNL's radiological hood with tube specimen (left) and tensile test setup (right) used in testing samples pre-charged with tritium

2.2.2 Smooth and Notched 304L Tensile Specimens

Samples of 304L stainless steel in the smooth tensile and notched tensile specimen geometries were supplied by SNL/CA. SRNL-STI-2020-00002 [13] documents the tritium precharging of forged 304L tensile specimens (both smooth and notched), and SRNL-STI-2021-00046 and in SRNL-STI-2022-00001 [8, 9] document details on the first and second rounds of testing at nominally 100 and 300 appm helium. The right panel of Figure 2-3 illustrates the test setup of the smooth specimen geometry, and Figure 2-4 shows the notched specimen. Additional specimens were further aged to approximately 650 appm helium before testing conducted to 5%, 10%, and 20% true strain as well as to failure. Notched tensile specimens were tested to a drop from peak load of 9% and 12%, as well as to failure. Notched tensile specimens exhibit triaxial stress states in testing, enabling the study of void nucleation. Smooth tensile specimen testing data informs the development of flow curves from tritium embrittled material for computational modeling. Interrupted tests were completed for microstructural characterization to advance understanding of deformation processes in tritium-exposed structural materials.

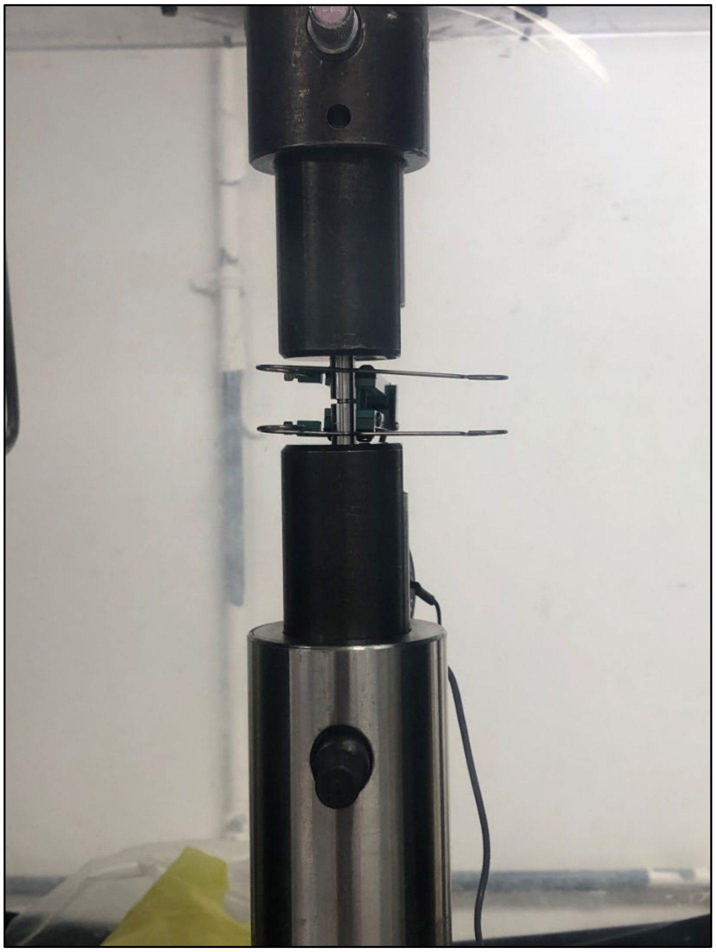

Figure 2-4 – Notched 304L specimen in testing configuration

2.3 Tensile testing of Annealed 21-6-9 material

SRNL-STI-2021-00046 [8] describes the preparation and thermal pre-charging with tritium of these annealed 21-6-9 stainless steel specimens. SRNL-STI-2022-00001 [9] describes initial testing at lower helium contents. Tensile tests on the annealed 21-6-9 specimens were conducted as described above. As above, tests were conducted to 5% and 20% true strain as well as to failure. Specimens were tested after accumulating 680 appm of decay helium.

2.4 New Sample Charging

Samples of additively manufactured 304L and 316L stainless steel were tritium pre-charged at the Savannah River Tritium Facility at the beginning of October, 2022. Included were smooth tensile specimens and arc shaped fracture mechanics specimens. A list of the charged specimens follows in Table 2-1.

Table 2-1 – Samples tritium pre-charged in October 2022

AM Stainless Steel Samples	Material	Quantity	Specimen ID
Smooth Tensile Geometry	304L	8	B1- 4,7,8,20 B2- 5,15,17,18
Smooth Tensile Geometry	316L	8	B3- 3,5,11,18 B4- 4,11,19,20
Arc Fracture Geometry	304L	8	B- 131,132,173,174,261,264,271,272
Arc Fracture Geometry	316L	8	B-351,354,361,363,421,424,444,461

After tritium charging, specimens were transferred to SRNL facilities for storage at -80°C. These charging conditions are predicted to yield initial concentrations of 3700 atomic parts per million tritium (appm) in 304L & 316L specimens, based on solubility calculations using data published by San Marchi et al [14]. Table 2-2 describes the notional plan for aging and testing these samples showing the storage times (aging) to reached desired He-3 levels.

Table 2-2 – Additively Manufactured 300 series stainless steel specimens test matrix

Test	# of Specimens			
	100 appm He (~6mo)	300 appm He (1.5 yr)	600 appm He (3 yr)	1000 appm He (5.6 yr)
Tensile to-failure (each alloy)	2	2	2	2
Arc Fracture Test (each alloy)	2	2	2	2

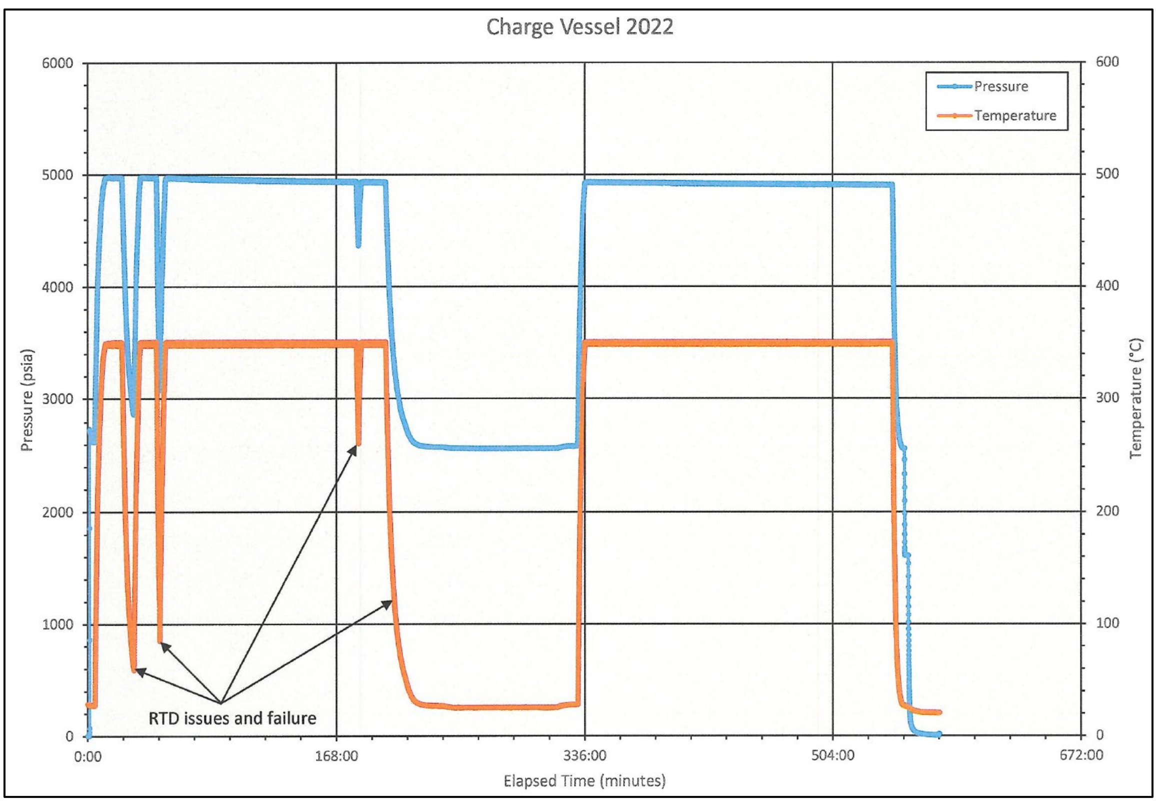

Figure 2-5 – 2022 Tritium charging run temperature and pressure record

3.0 Results and Discussion

3.1 Fracture testing of 304L EB welds

Fracture resistance testing was conducted per ASTM E1820 on a second aging of EB welded 304L stainless steel arc shaped fracture mechanics specimens. Due to delays in computer, camera, and software upgrades to the contaminated specimen imaging capability, a full J-integral analysis of the specific energy versus crack extension has been deferred into 2023. Thus, for qualitative comparison, load curves normalized to test peak loads are displayed versus crack opening displacement (COD) in Figure 3-1 for both the 300 appm helium testing and the 100 appm testing conducted in prior years. This indicates a degree of embrittlement in the generally reduced extension to peak load and more rapid drop off of load sustained over the test.

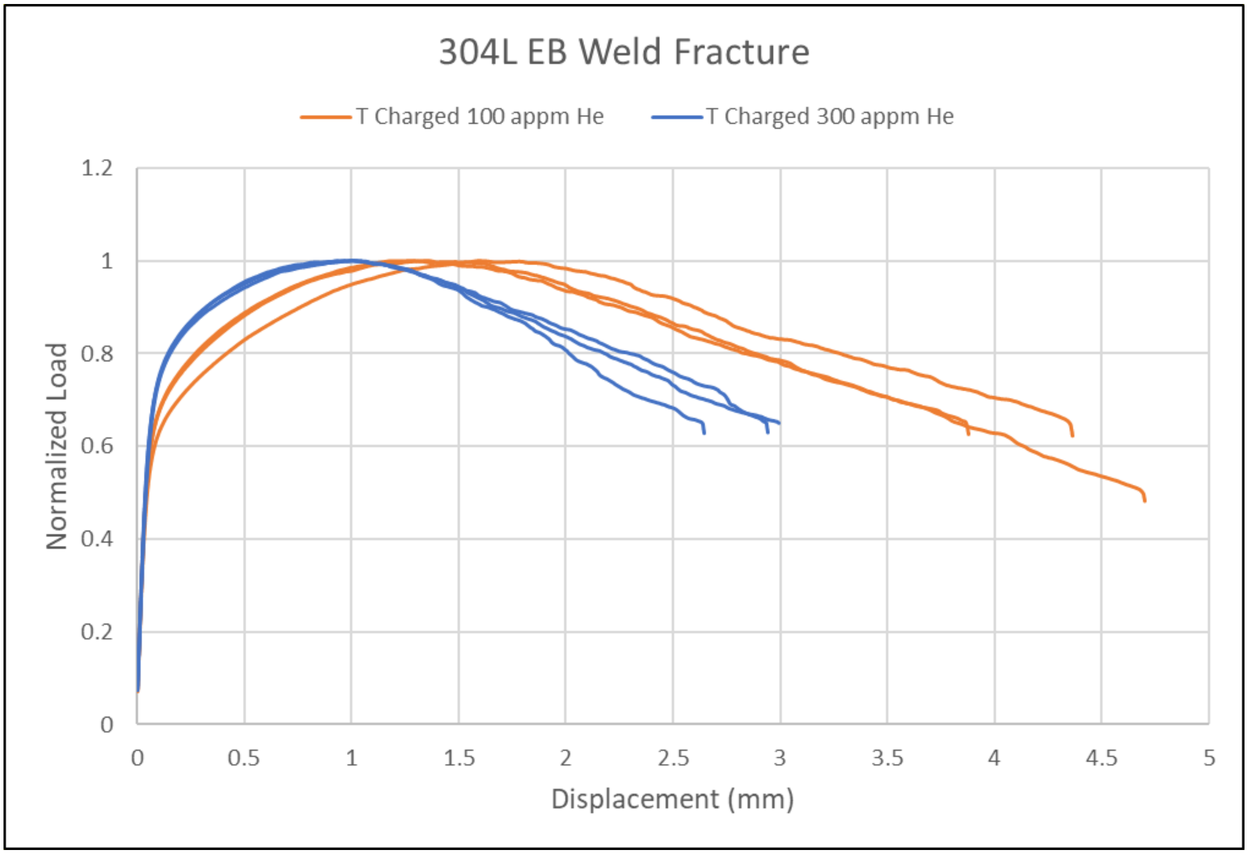

Figure 3-1 – Load versus crack opening displacement curves measured for tests with EB weld material thermally pre-charged with nominally 3700 appm tritium and aged to develop nominally 100 and 300 appm of helium

3.2 Tensile Testing Results from 304L EB welds

Engineering stress strain curves from the tensile testing of EB weld specimens thermally pre-charged with tritium and aged to 300 appm of helium are shown in Figure 3-2 in comparison to specimens tested at 100 appm helium. This chart reveals the expected increase in yield strength with increasing helium ingrowth. Shown in Figure 3-3 are the yield strength and ultimate tensile strength values (left) and reduction in area values (right). The numerical values are also documented in Appendix A.

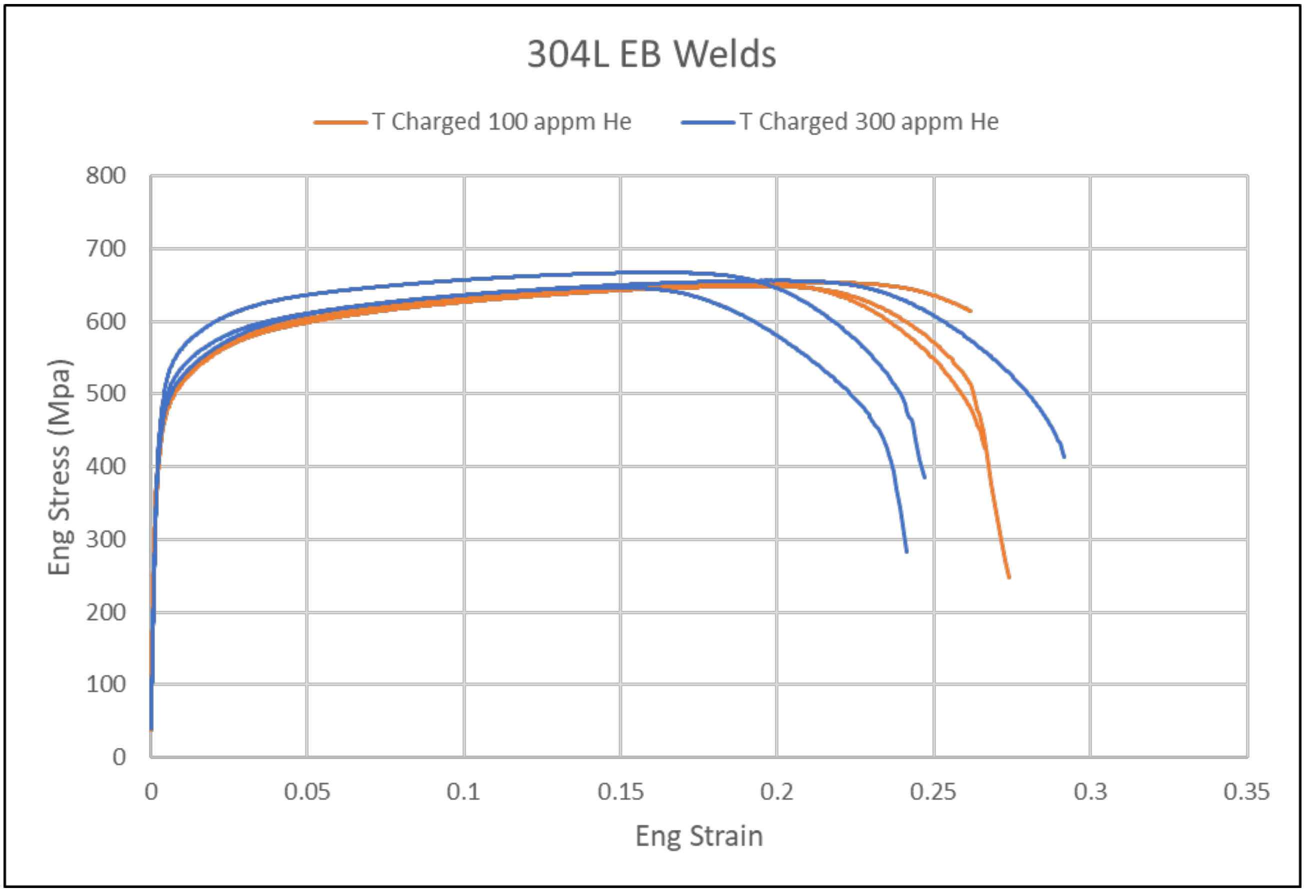

Figure 3-2 – Engineering stress strain curves from tests with EB weld material thermally pre-charged with nominally 3700 appm tritium and aged to develop nominally 300 appm of helium, compared to previously tested specimens from the same charging aged to 100 appm helium

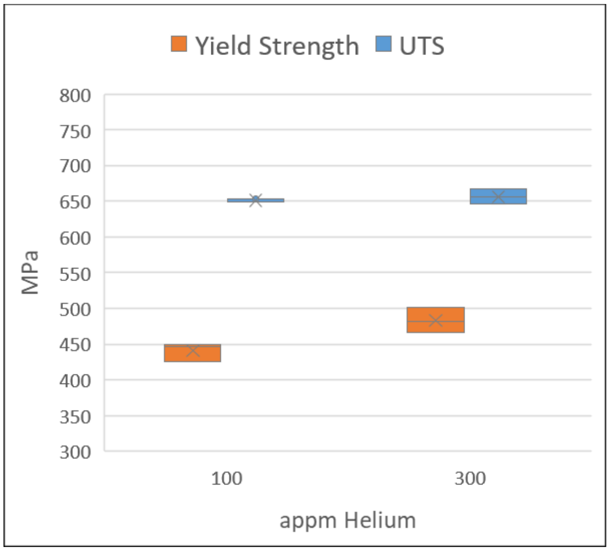

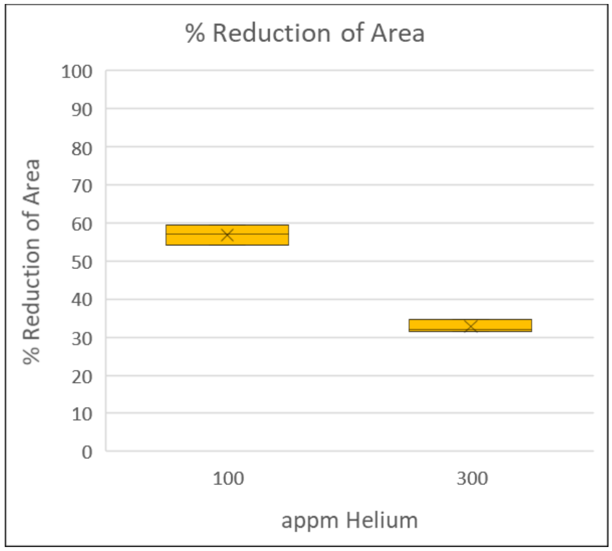

Figure 3-3 – Yield Strength, Ultimate Tensile Strength (left) and Percent Reduction in Area (right) in EB welded 304L stainless steel after pre-charging with tritium and aging to 100 and 300 appm helium

3.3 Testing Results from 304L Material

3.3.1 304L Tube Specimens

For reference, the microstructures of the as-received and heat treated materials are shown in Figure 3-4.The heat treatments used to create these microstructures were described previously in [12].

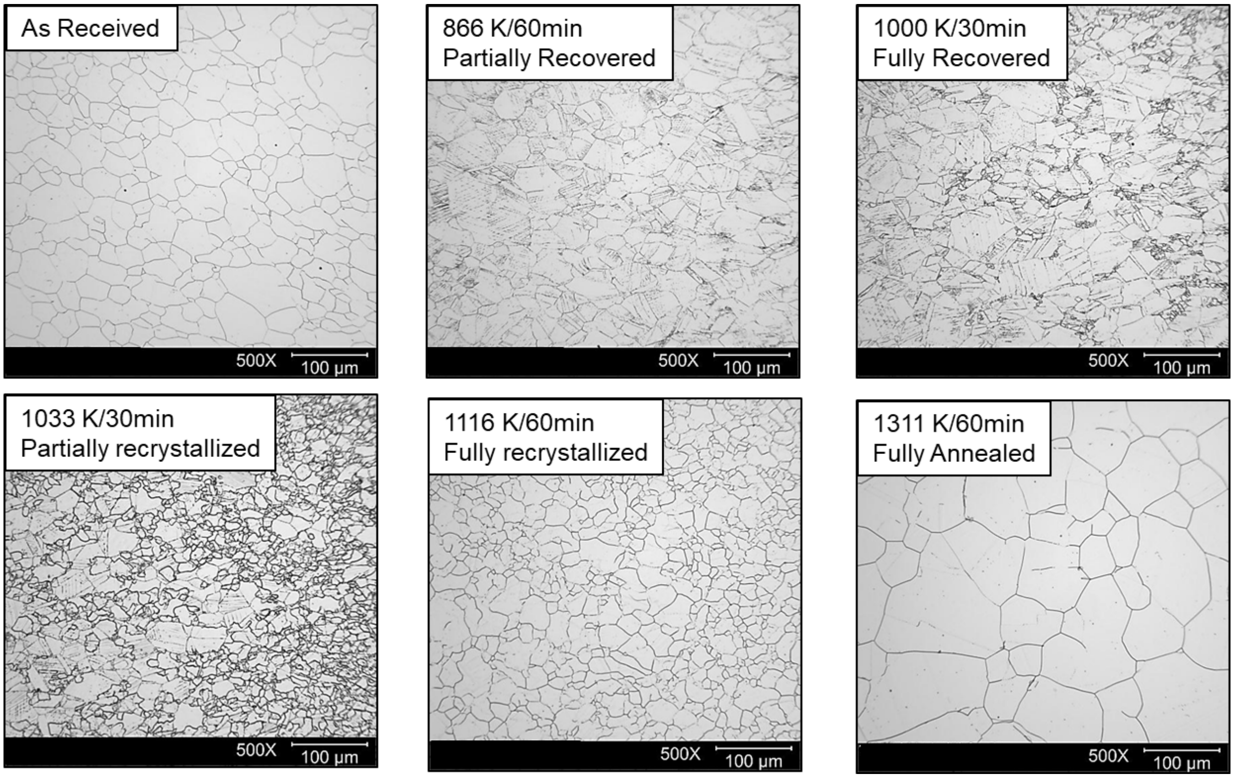

Figure 3-4 – Micrographs of 304L tube microstructures based on different heat treatments. Reproduced with permission from SNL/CA through SAND2020-8528 PE [15]

Figure 3-5 displays Stress-Strain curves from two of the above microstructures, the As-Received, and Fully Recrystallized material. For each microstructure, testing was conducted on the uncharged, hydrogen-precharged, and several tritium-precharged-and-aged conditions, including ages resulting in 100, 300, and 650 appm helium. It is clear that the heat treatment is a dominating factor on mechanical response, over that of the hydrogen isotope. Additionally, the heat treatment leads to differing sensitivity to hydrogen isotope embrittlement. It is important to note that the hydrogen pre-charging conditions resulted in a nominal hydrogen content of 7700 appm, while the tritium-aged condition resulted in nominally 3600 appm of tritium. Thus, at low helium content, a larger effect of hydrogen should be expected, and is seen in both materials. This trend continues through all ages of the As-received microstructure, however, in the Fully Recrystallized material, larger amounts of decay helium more than make up the difference in initial hydrogen isotope content, and eventually significantly more hardening is seen in the longest aged tritium-exposed specimens when 650 appm helium accumulates. Figure 3-6 displays collected yield strength information for each microstructure and exposure condition, averaged over all the tested repeats. The same microstructural dependence on the sensitivity to hydrogen and helium embrittlement is see in total in this chart.

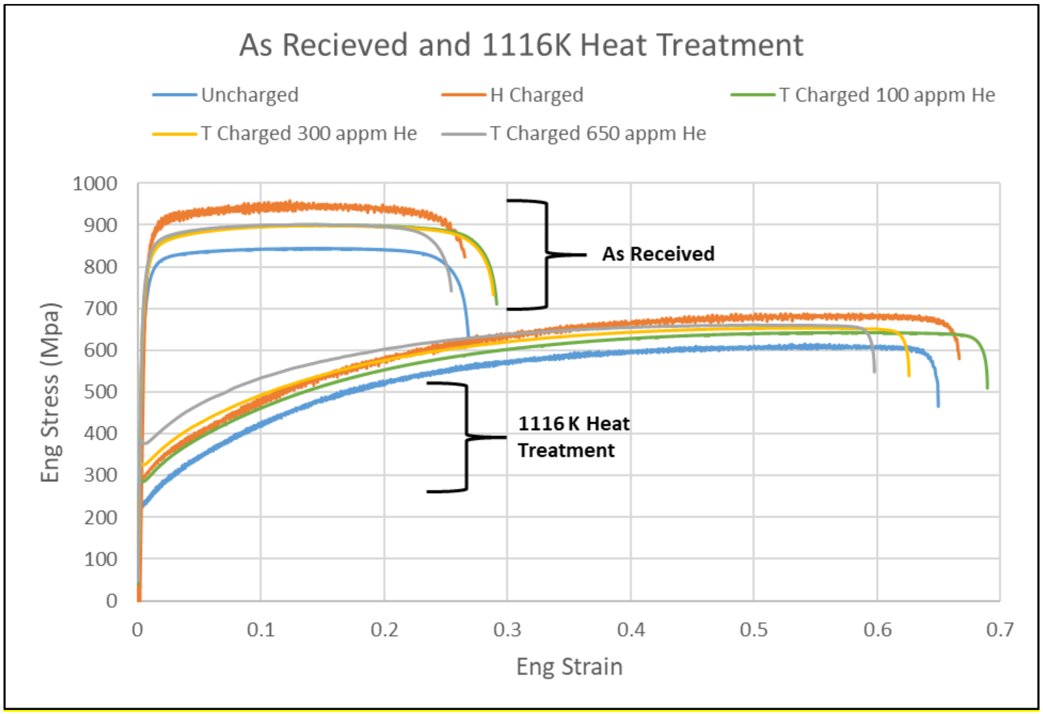

Figure 3-5 – Engineering Stress / Strain data from the As-Received (strain hardened) and 1116K (fully recrystallized) microstructures at each condition

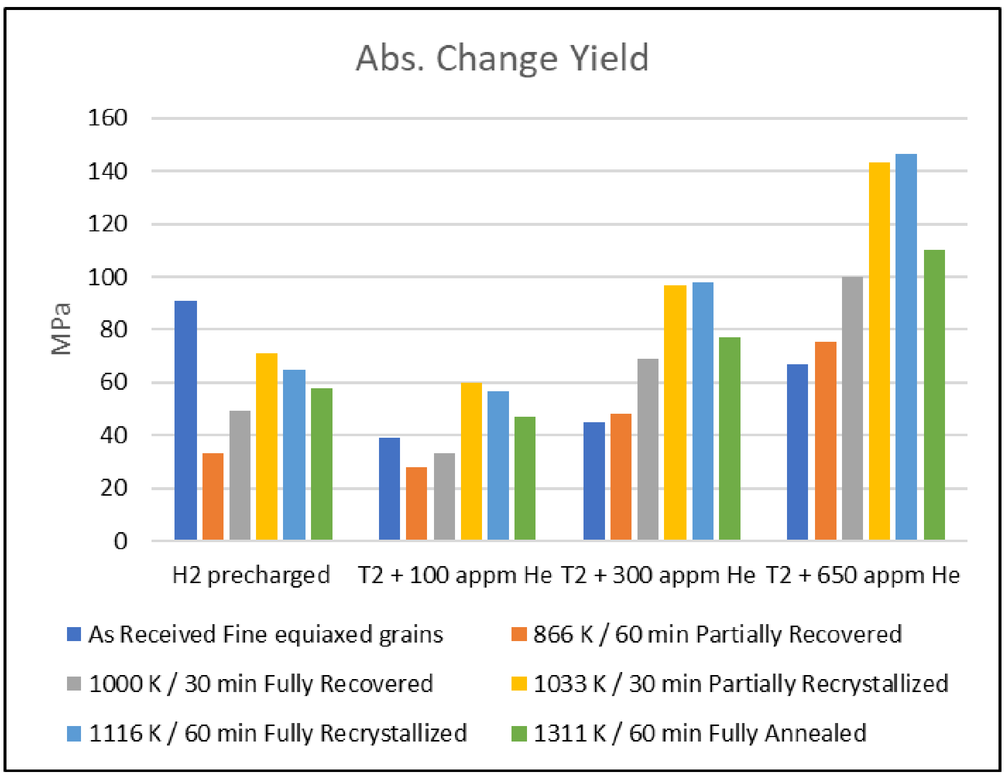

Figure 3-6 – Absolute change (from the uncharged control) in yield in MPa for each material condition of 304L tubes

Figure 3-7 displays the reduction in diameter for each tube microstructure and exposure condition. Typically, reduction in area (for which reduction in diameter is a proxy due to the tube geometry) is a good qualitative correlate of ductility loss. Thus, the apparent stronger effect of modest amounts of decay helium over that of pure hydrogen might suggest an area for further investigation with fracture mechanics testing. These behaviors are related to the fundamental mechanisms of embrittlement from each species and their interactions with each other, which are still poorly understood.

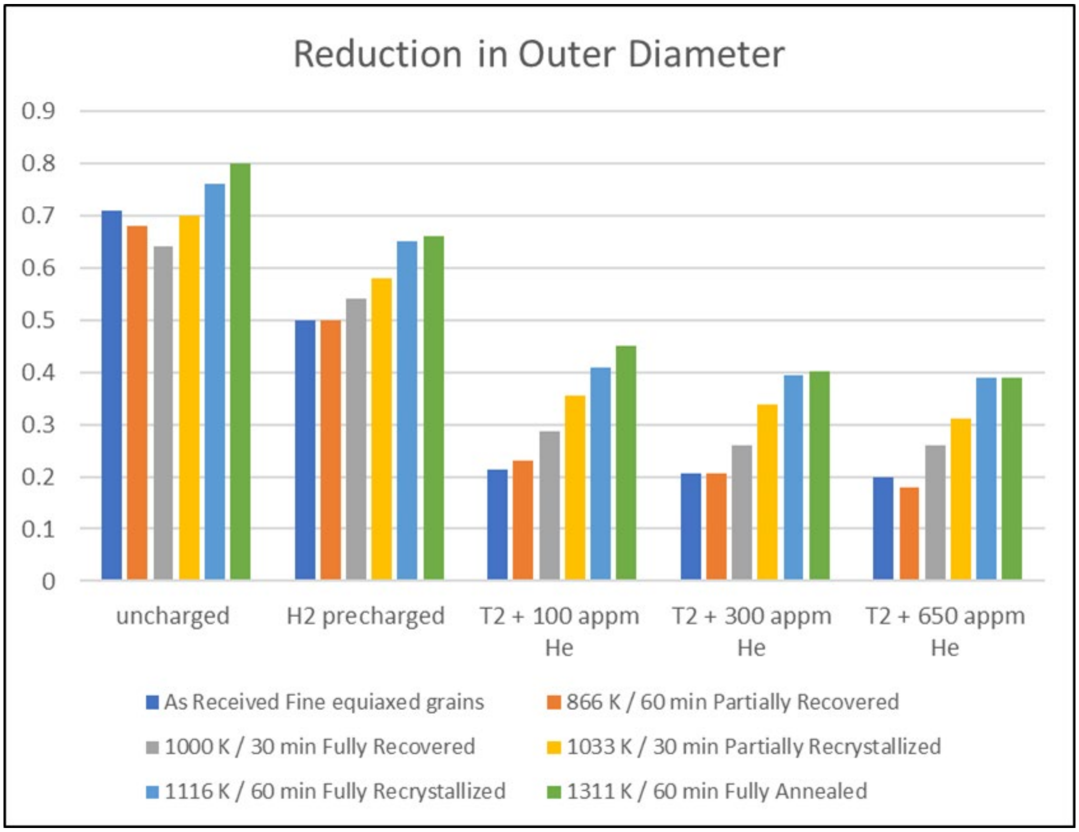

Figure 3-7 – Reduction in outer diameter for each material condition of 304L tubes

3.3.2 304L notched and smooth tensile tests

Below are plots of the tensile test results from both notched [Figure 3-8] and smooth [Figure 3-9] 304L specimens. Engineering stress versus strain is shown for the smooth tensile geometry, while load versus displacement is shown for the notched geometry, where uniaxial stresses are inapplicable. Both of these geometries in their tests to failure and interrupted testing generate data for modeling efforts, as well as specimens for microstructural characterization. The first of these microstructural studies are planned for 2023. From the smooth tensile specimens, yield strength, ultimate tensile strength, and reduction in area were also calculated, and these are summarized in [Figure 3-10] and documented in Appendix A.

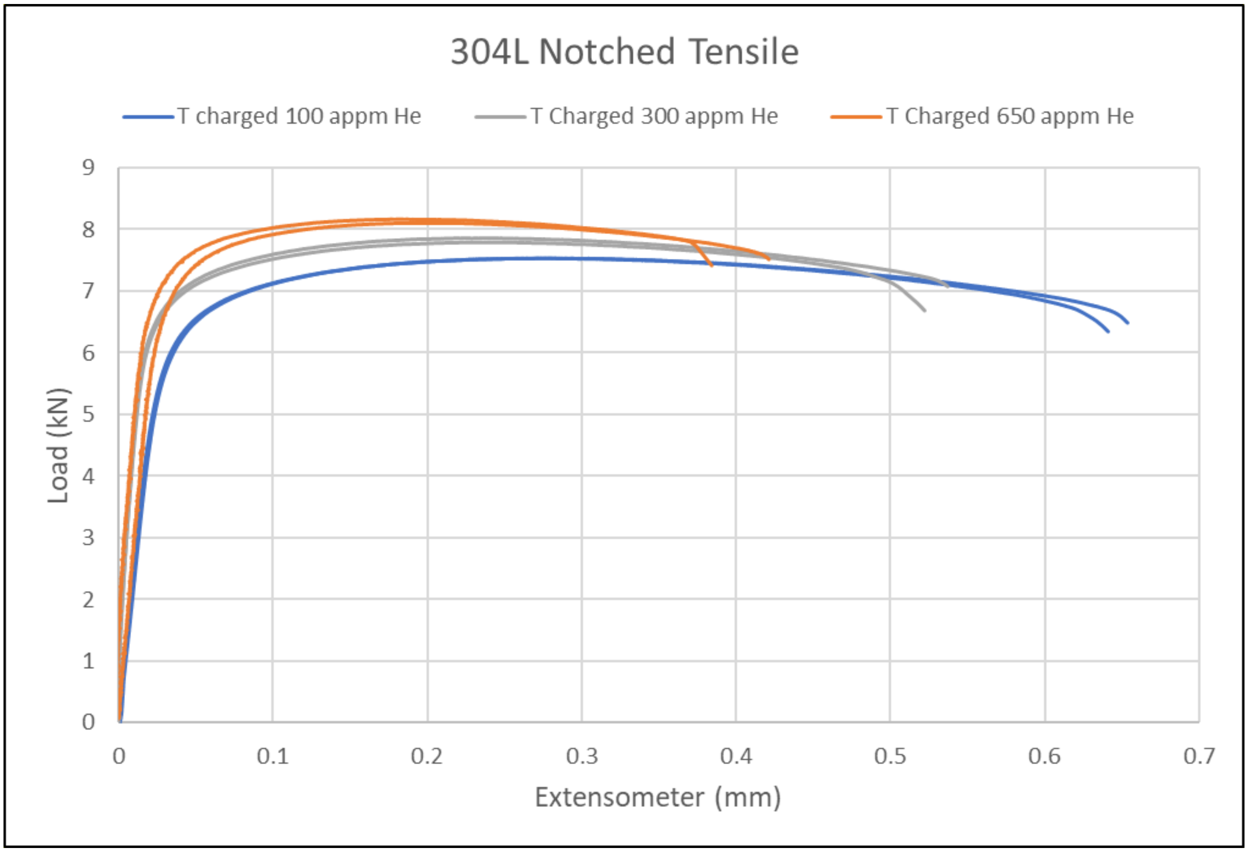

Figure 3-8 – Load / Extension curves for each tested condition to date of notched 304L specimens

3.4 Tensile Testing of annealed 21-6-9 material

Figure 3-11 display the tensile test results from annealed 21-6-9 alloy specimens tested with 680 appm accumulated helium. It is presented with prior testing results at 100, 200, and 300 appm helium. Yield strength, ultimate tensile strength, and reduction in area were calculated, and are shown in [Figure 3-12] and documented in Appendix A. These annealed 21-6-9 specimens are being used as a model to compare to the heat affected zone of welds in forged 21-6-9 to make simpler the testing of material with similar thermal histories and microstructures to in-service welds.

3.5 Sub-Ambient Mechanical Testing Capability

A new sub-ambient test chamber and associated chiller have been received at SRNL (see Figure 3-13). This equipment will support the Aging and Lifetimes program by providing testing capabilities for tritium charged materials at sub-ambient temperatures not previously available. Prior to installation, the test chamber and chiller will be evaluated for performance. Clean testing of the test chamber is planned to occur in 2023.

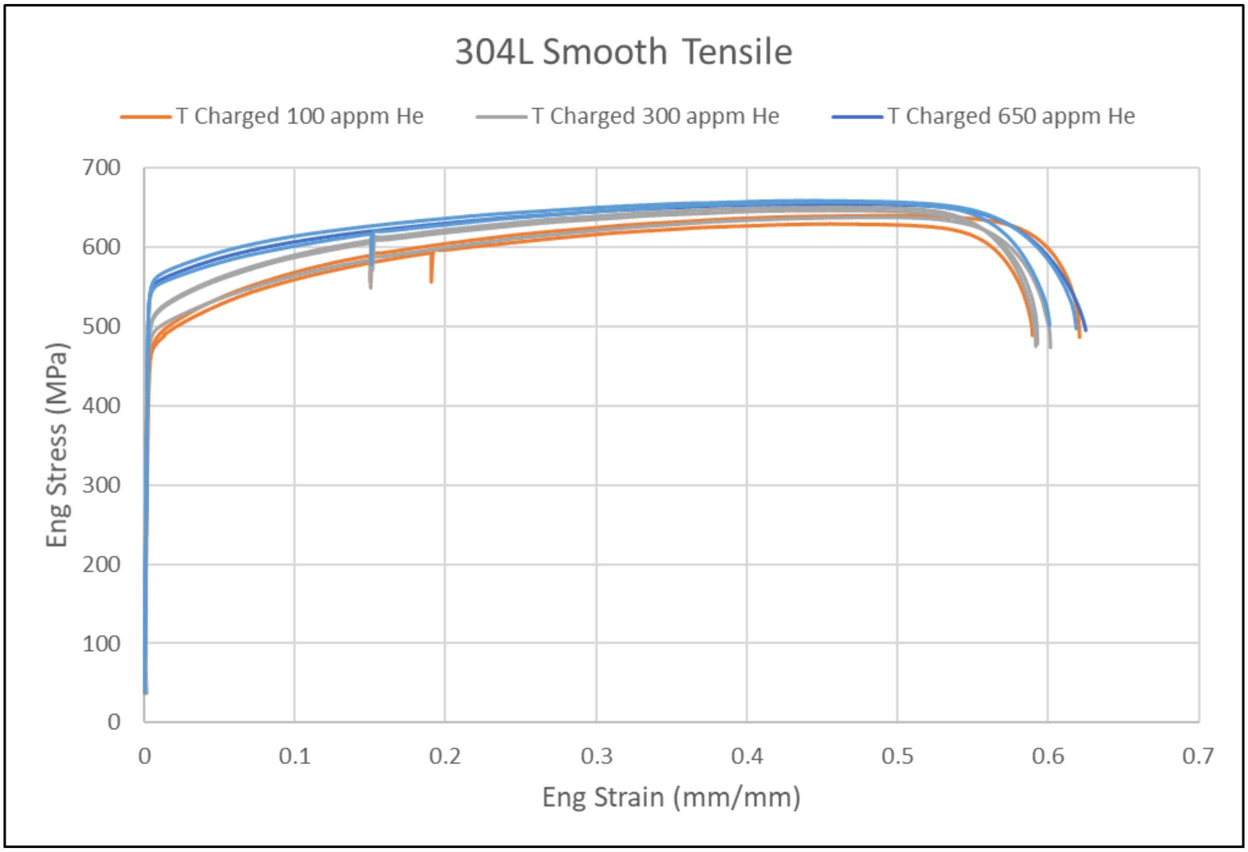

Figure 3-9 – Engineering Stress / Strain curves for each tested condition to date of 304L specimens

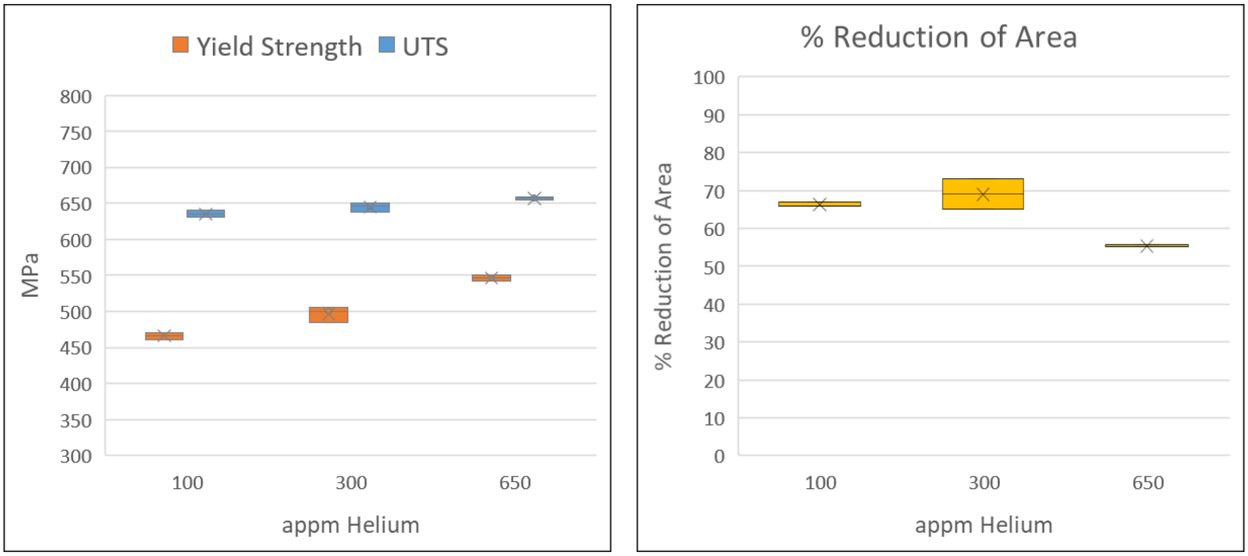

Figure 3-10 – Collected Yield Strength, Ultimate Tensile Strength (left) and Percent Reduction in Area (right) in 304L stainless steel after pre-charging with tritium and aging to 100, 300, and 650 appm helium

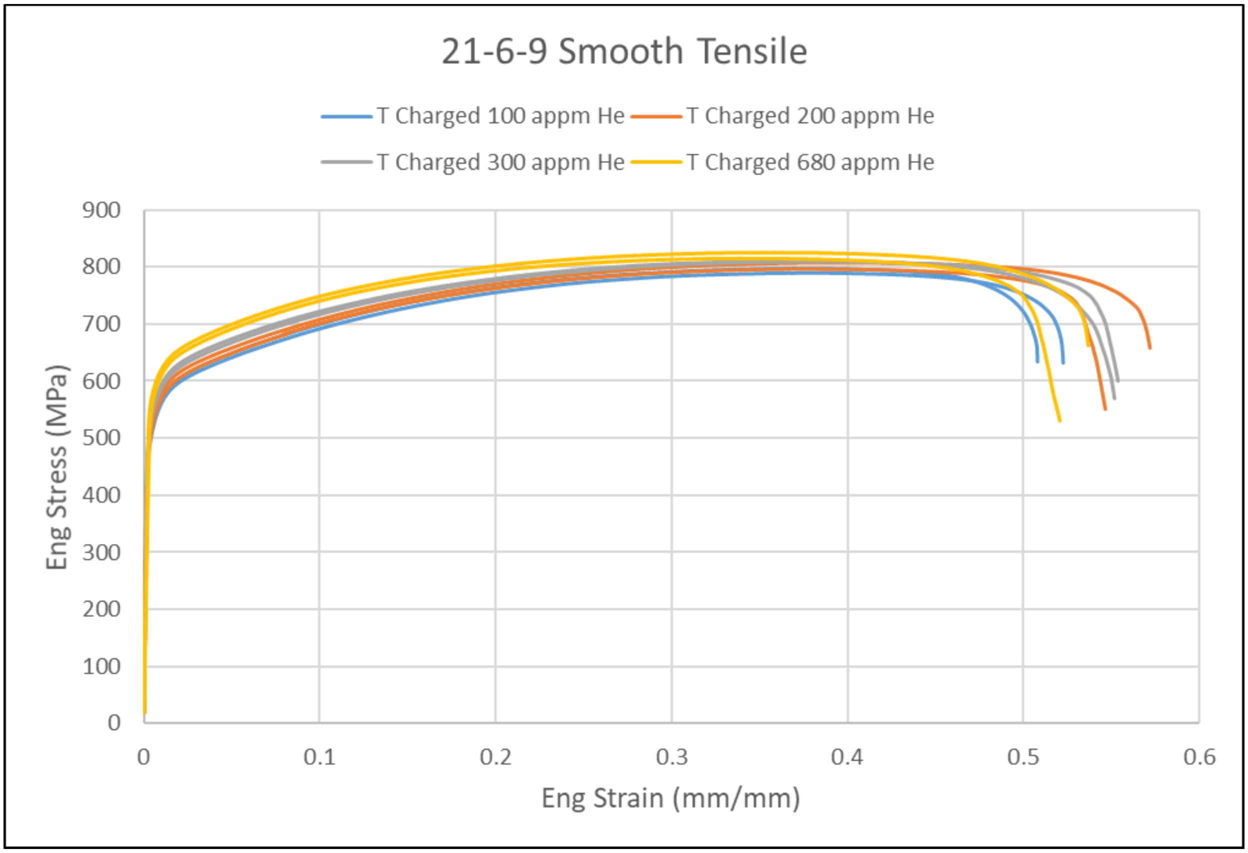

Figure 3-11 – Engineering Stress / Strain curves for all tested conditions of 21-6-9 specimens

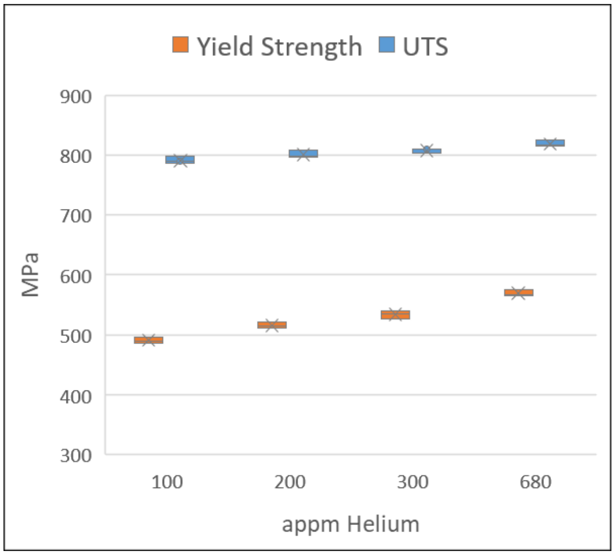

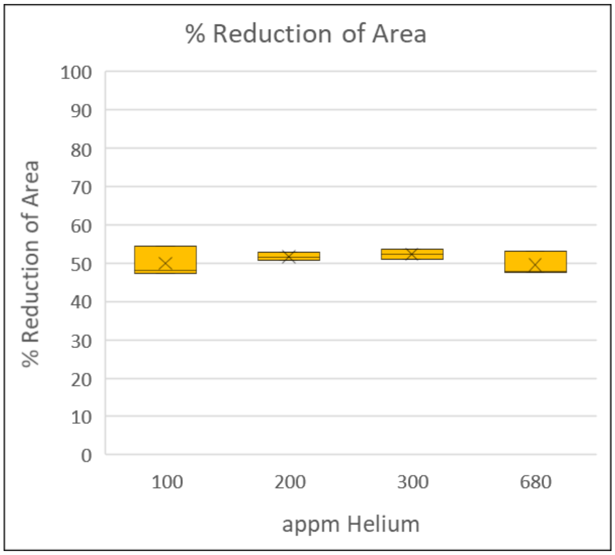

Figure 3-12 – Collected Yield Strength, Ultimate Tensile Strength (left) and Percent Reduction in Area (right) in 21-6-9 stainless steel after pre-charging with tritium and aging

Figure 3-13 – Pictures of test chamber (left) and chiller (right) for sub-ambient mechanical testing of tritium contaminated specimens

4.0 Conclusions

- The 3-year testing plan for the 304L tubes microstructure study started in 2019 was completed on schedule. The microstructural dependence of each material to tritium embrittlement has now been measured from low to high helium contents, and further microscopy is being considered to explore the underlying deformation mechanisms will be required to construct quantitative structure-property relationships
- 304L forged and EB weld smooth tensile testing was completed at 650 and 300 appm helium respectively. Each material displayed the anticipated hardening and loss of ductility with increasing aging. Interestingly, when comparing the EB welded material to the prior testing data of the forged material, the relative effects of tritium-decay-helium was enhanced, suggesting higher sensitivity of the welds to tritium embrittlement. Upcoming analysis of fracture mechanics testing on EB welded 304L material will quantify what if any impact this has on measured fracture resistance.
- A 4^{th} round of tensile testing was completed on annealed 21-6-9 stainless steel, expanding on work started in 2021 to investigate the larger than expected embrittlement in the heat affected zones of welds in the 21-6-9 forgings. While furthered hardening was measured, and ductility decreased, these tensile tests alone have not sufficed to explain the measured decreases in fracture resistance, and further work is planned, both in long aged 21-6-9 welds and a new study is planned to allow for fracture mechanics testing at lower helium contents to further investigate this phenomenon
- Work to establish sub-ambient testing capabilities at SRNL suited for handling tritium contaminated material continues. The custom-engineered environmental chamber and chiller unit have been received and are planned to be initially proved with clean material in 2023.

5.0 References

[1] G. R. Caskey, "Hydrogen Effects in Stainless Steel," in *Hydrogen Degradation of Ferrous Alloys*, R. A. Oriani, J. P. Hirth, and M. A. Smialowski, Eds., ed Park Ridge, NJ: Noyes Publishing, 1985, pp. 822-862.

[2] G. Caskey Jr, "Tritium-helium effects in metals," *Fusion Technology,* vol. 8, pp. 2293-2298, 1985.

[3] S. L. Robinson and G. J. Thomas, "Accelerated Fracture due to Tritium and Helium in 21-6-9 Stainless Steel," *Metallurgical Transactions A,* vol. 22A, pp. 879-885, 1991.

[4] S. L. Robinson, "The Effects of Tritium on the Flow and Fracture Stress of Austenitic Stainless Steels," in *Hydrogen Effects on Material Behavior*, N. R. Moody and A. W. Thompson, Eds., ed Warrendale PA: TMS, 1990, pp. 433-445.

[5] S. Robinson and N. Moody, "The effect of hydrogen, tritium and decay helium on the fracture toughness of a stainless steel superalloy," *Journal of Nuclear Materials,* vol. 140, pp. 245-251, 1986.

[6] M. J. Morgan, D. Hitchcock, T. Krentz, J. McNamara, and A. Duncan, "2017 Accomplishments–Tritium Aging Studies on Stainless Steel Weldments and Heat-Affected Zones," SRNL-STI-2018-00036 Savannah River Site (SRS), Aiken, SC (United States)2018.

[7] T. M. Krentz, D. A. Hitchcock, M. J. Morgan, J. A. Ronevich, R. Sills, C. San Marchi*, et al.*, "Fracture Toughness Properties of Tritium-Charged-and-Aged Stainless Steels: SRNL and SNL Collaboration Test Plan and 2018 Results," SRNL-STI-2019-00022 Savannah River National Laboratory, Aiken, SC (United States)2019.

[8] T. M. Krentz, "2020 Report-SRNL Aging and Lifetimes program tritium aging studies on structural alloys," Savannah River Site (SRS), Aiken, SC (United States). SRNL-STI-2021-00046, 2021.

[9] T. M. Krentz and A. Mullins, "2021 REPORT - SRNL AGING AND LIFETIMES PROGRAM TRITIUM AGING STUDIES ON STRUCTURAL ALLOYS," Savannah River National Lab, Aiken, SC SRNL-STI-2022-00001, 2022.

[10] L. A. Hughes, B. P. Somerday, D. K. Balch, and C. San Marchi, "Hydrogen Compatibility of Austenitic Stainless Steel Tubing and Orbital Tube Welds," in *International Conference on Hydrogen Safety (ICHS)*, Brussels, Belgium, 2013.

[11] L. A. Hughes, B. P. Somerday, D. K. Balch, and C. San Marchi, "Hydrogen compatibility of austenitic stainless steel tubing and orbital tube welds," *International Journal of Hydrogen Energy,* vol. 39, pp. 20585-20590, 2014.

[12] T. K. Krentz, J. A. Ronevich, D. K. Balch, and C. San Marchi, "Tritium embrittlement of austenitic stainless-steel tubing at low helium contents," *Manuscript Submitted for Publication,* 2020.

[13] T. Krentz and D. Hitchcock, "2019 ACCOMPLISHMENTS-DEGRADATION OF MECHANICAL PROPERTIES IN STRUCTURAL METALS AND WELDS FOR GTS RESERVOIRS," Savannah River National Laboratory SRNL-STI-2020-00002, 2020.

[14] C. San Marchi, B. P. Somerday, and S. L. Robinson, "Permeability, Solubility, and Diffusivity of Hydrogen Isotopes in Stainless Steels at High Gas Pressures," *International Journal of Hydrogen Energy,* vol. 32, pp. 100-116, 2007.

[15] L. A. Hughes and e. al, "Hydrogen Effects on 304L Tubing as a Function of Microstructure," Sandia National Laboratories SAND2020-8528 PE.

6.0 Appendices

Appendix A. Tabulated Results from Tensile Testing

Table 6-1 – Mechanical Properties of Electron Beam Welded 304L Stainless Steel

Environmental condition (appm)	Yield Strength (MPa)	Tensile Strength (MPa)	Total Elongation (%)	Reduction of Area
T + 100 He	440 ± 12	651 ± 2.3	27	0.57 ± 0.027
T + 300 He	483 ± 17.5	656 ± 10.2	33	0.33 ± 0.015

Table 6-2 – Mechanical Properties of 304L Smooth Tensile Specimens

Environmental condition (appm)	Test length	Yield Strength (MPa)	Tensile Strength (MPa)	Total Elongation (%)	Reduction of Area
T + 100 He	5% True Strain	471	536	5	nm
	10% True Strain	477	575	11	nm
	20% True Strain	478	605	15	nm
	To Failure	466 ± 5	635 ± 5	58 ± 3.5	0.66 ± 0.005
T + 300 He	5% True Strain	506 ± 1.5	560 ± 0.2	5	nm
	10% True Strain	502 ± 3	586 ± 3.5	11	nm
	20% True Strain	497 ± 2	613 ± 1	21	nm
	To Failure	497 ± 10	645 ± 6	59 ± 0.5	0.69 ± 0.04
T + 650 He	5% True Strain	549 ± 0.5	590 ± 0.5	5	nm
	10% True Strain	551 ± 0.5	613 ± 0.6	11	nm
	20% True Strain	551 ± 1	640 ± 1.6	22	nm
	To Failure	546 ± 4.5	657 ± 1.9	63 ± 2.5	0.55 ± 0.004

Table 6-3 – Mechanical Properties of 304L Tubing

Includes hydrogen test data from SNL/CA, reproduced from [12]
*Note: RA values for Tritium pre-charged specimens correspond to reduction in outer diameter measurements, which might not perfectly reflect reduction in area in a tube specimen geometry.

Microstructure	Environmental condition (appm)	Yield Strength (MPa)	Tensile Strength (MPa)	Total Elongation (%)	Reduction of Area*
Strain-hardened (as-received)	Non-charged	697	857	23	0.71
	H-precharged	788	945	27	0.50
	T + 100 He	802 ± 63	907 ± 5	27	0.21 ± 0.023
	T + 300 He	742	898 ± 0.3	29	0.20 ± 0.022
	T + 650 He	764	902 ± 1	27 ± 1.5	0.20 ± 0.01
Partially recovered	Non-charged	678	854	27	0.68
	H-precharged	711	915	32	0.50
	T + 100 He	706 ± 6.5	874 ± 0.3	34	0.23 ± 0.023
	T + 300 He	726 ± 6.5	880 ± 0.1	33.5 ± 1	0.20 ± 0.002
	T + 650 He	753 ± 2.5	880 ± 1	30 ± 1	0.18 ± 0.002
Fully recovered	Non-charged	576	780	36	0.64
	H-precharged	625	850	41	0.54
	T + 100 He	609 ± 0.5	798 ± 0.3	45 ± 0.5	0.29 ± 0.015
	T + 300 He	645 ± 3.5	808 ± 3	45 ± 1	0.26 ± 0.032
	T + 650 He	676 ± 3	810 ± 3	41 ± 1.5	0.26 ± 0.002
Partially recrystallized	Non-charged	377	692	47	0.70
	H-precharged	448	770	53	0.58
	T + 100 He	437 ± 1	726 ± 0.4	54 ± 1	0.36 ± 0.007
	T + 300 He	470 ± 0.5	732 ± 0.3	51.5 ± 3	0.34 ± 0.07
	T + 650 He	520 ± 5	735 ± 3	51	0.31 ± 0.01
Fully recrystallized	Non-charged	228	614	63	0.76
	H-precharged	293	688	67	0.65
	T + 100 He	285 ± 1	641 ± 1.3	69 ± 0.5	0.41
	T + 300 He	326 ± 0.5	650 ± 1.2	46.5 ± 3	0.39 ± 0.005
	T + 650 He	374 ± 2.5	655 ± 0.2	43 ± 3	0.39 ± 0.007
Annealed	Non-charged	179	565	64	0.80
	H-precharged	237	636	71	0.66
	T + 100 He	226 ± 1	593 ± 0.4	74 ± 1.5	0.45 ± 0.026
	T + 300 He	255 ± 0.5	587 ± 0.5	44	0.40 ± 0.032
	T + 650 He	289 ± 1	595 ± 0.04	42 ± 1	0.39 ± 0.013

Table 6-4 – Mechanical Properties of Welded 304L Tubing

Includes hydrogen test data from SNL/CA for completeness, reproduced from [12]
*Note: RA values for Tritium pre-charged specimens correspond to reduction in outer diameter measurements, which might not perfectly reflect reduction in area in a tube specimen geometry.

Microstructure	Environmental condition (appm)	Yield Strength (MPa)	Tensile Strength (MPa)	Total Elongation (%)	Reduction of Area*
As-received tubing welded	Non-charged	248	566	15	0.82
	H-precharged	287	631	15	0.62
	T + 100 He	287 ± 0.5	600 ± 0.6	15 ± 1	0.28 ± 0.017
	T + 300 He	314 ± 5	606 ± 1.5	13.5 ± 2	0.26 ± 0.023
	T + 650 He	345 ± 3.5	618 ± 4.5	14	0.27 ± 0.04
fully recovered tubing welded	Non-charged	256	577	16	0.82
	H-precharged	296	651	15	0.67
	T + 100 He	281 ± 1	594 ± 0.5	15	0.29 ± 0.006
	T + 300 He	311 ± 3	608 ± 0.17	n/m	0.31 ± 0.004
	T + 650 He	344 ± 5.5	618 ± 0.3	14 ± 1	0.24 ± 0.002
annealed tubing welded	Non-charged	178	561	59	0.78
	H-precharged	239	630	67	0.65
	T + 100 He	239	601	68	0.43
	T + 300 He	260 ± 1	586 ± 2.7	n/m	0.40 ± 0.007
	T + 650 He	296	604 ± 6.3	46 ± 4	0.38

Table 6-5 – Mechanical Properties of Annealed 21-6-9 Stainless Steel

Environmental condition (appm)	Test length	Yield Strength (MPa)	Tensile Strength (MPa)	Total Elongation (%)	Reduction of Area
T + 100 He	5% True Strain	498 ± 2.7	645 ± 4.3	5	0.05 ± 0.003
	20% True Strain	492 ± 5.5	750 ± 15	19 ± 1.2	0.16 ± 0.017
	To Failure	491 ± 5.3	791 ± 5.6	55 ± 6.1	0.50 ± 0.036
T + 200 He	5% True Strain	511 ± 0.7	651 ± 1.8	5	n/m
	20% True Strain	513 ± 7.6	771 ± 3	22	n/m
	To Failure	516 ± 4.2	800 ± 5.5	54 ± 3.1	0.52 ± 0.01
T + 300 He	5% True Strain	533 ± 1	666 ± 2	5	0.04 ± 0.003
	20% True Strain	538 ± 0.1	783 ± 2.5	22	0.17 ± 0.003
	To Failure	534 ± 6.8	807 ± 4	55 ± 0.3	0.52 ± 0.013
T + 680 He	5% True Strain	555	676	5	n/m
	20% True Strain	552	787	22	n/m
	To Failure	570 ± 5	819 ± 5	58 ± 2.5	0.50 ± 0.03